

## **New statistical quantification of the impact of active deformation on the distribution of submarine channels**

**Tracking no:** G48698R

**Authors:**

Marco Pizzi (Imperial College), Alexander Whittaker (Imperial College), Lonergan Lidia (Imperial College), Mike Mayall (Imperial College), and W. Mitchell (Imperial College)

**Abstract:**

Submarine channel systems play a crucial role in governing the delivery of sediments and pollutants such as plastics from the shelf edge to deep-water. Understanding their distribution in space and time is important to constrain the locus, magnitude and characteristics of deep-water sedimentation, and to predict stratigraphic architectures and depositional facies. Using 3D seismic reflection data covering the outer fold and thrust belt of the Niger Delta, we determined the pathways of Miocene to Pliocene channels that crossed eleven fold-thrust structures, at 173 locations, for which the temporal and spatial evolution of strain rates have been constrained over 11 My. We use a statistical approach to quantify strain and shortening rate distributions recorded where channels have crossed structures, compared to the fault array as a whole. Our results prove unambiguously that these distributions are different. The median strain rate where channels cross faults is  $< 0.6\%/My$  ( $\sim 40m/My$ ), 2.5 times lower than the median strain rate of active fault segments ( $1.5\%/My$ ) with a marked reduction in the number of channel-fault crossings where fault strain rates exceed  $1\% Ma$ . Our results quantify the sensitivity of submarine channels to active deformation at a population level for the first time, and enable us to predict the temporal and spatial routing of submarine channels affected by structurally-driven topography.

# **New statistical quantification of the impact of active deformation on the distribution of submarine channels**

Marco Pizzi<sup>1,2</sup>, Alexander C. Whittaker<sup>1\*</sup>, Lidia Lonergan<sup>1</sup>, Mike Mayall<sup>1</sup>, W. Hamish Mitchell<sup>1</sup>.

<sup>1</sup>Department of Earth Science & Engineering, Imperial College, London SW7 2AZ, UK.

\*Corresponding author.

<sup>2</sup>*now at*: Fugro GB Marine Limited, Victory House, Trafalgar Wharf (Unit 16), Hamilton Road, Portsmouth, PO6 4PX, UK.

## **ABSTRACT**

Submarine channel systems play a crucial role in governing the delivery of sediments and pollutants such as plastics from the shelf edge to deep-water. Understanding their distribution in space and time is important to constrain the locus, magnitude and characteristics of deep-water sedimentation, and to predict stratigraphic architectures and depositional facies. Using 3D seismic reflection data covering the outer fold and thrust belt of the Niger Delta, we determined the pathways of Miocene to Pliocene channels that crossed eleven fold-thrust structures, at 173 locations, for which the temporal and spatial evolution of strain rates have been constrained over 11 My. We use a statistical approach to quantify strain and shortening rate distributions recorded where channels have crossed structures, compared to the fault array as a whole. Our results prove unambiguously that these distributions are different. The median strain rate where channels cross faults is  $< 0.6\%/My$  ( $\sim 40m/My$ ), 2.5 times lower than the median strain rate of active fault segments ( $1.5\%/My$ ) with a marked reduction in the number of channel-fault crossings where fault strain rates exceed  $1\% Ma$ . Our results quantify the sensitivity of submarine channels to active deformation at a population level for the first time, and enable us to predict the temporal and spatial routing of submarine channels affected by structurally-driven topography.

## **INTRODUCTION**

Submarine channel systems form the largest sedimentary deposits on Earth (Talling et al., 2015) and control the delivery of sediment, organic material and plastics from the continents to deep water (Babonneau et al., 2002; Covault et al., 2016; Sweet and Blum, 2016; Kane & Clare, 2019). Understanding their distribution in space and time is important to constrain the

36 locus, magnitude and completeness of deep-water stratigraphy, and to predict stratigraphic  
37 architectures and reservoir facies (Mayall et al., 2006, 2010; Sømme et al. 2009; Covault et  
38 al., 2016). Submarine channels are often found on passive margins that deform due to gravity  
39 tectonics, causing the growth of folds and thrusts at the toe-of-slope (Damuth 1994; Corredor  
40 et al 2005; Jolly et al., 2016; Don et al., 2019). The growth of these structures is expressed by  
41 the creation of seabed topography that modifies the slope gradient and creates tortuous  
42 corridors, which can be exploited by the channels (Smith, 2004; Callec et al., 2010; Bourget  
43 et al., 2011; Howlett et al., 2019) (Fig 1). Although it is often assumed that submarine  
44 channels are sensitive to topographic changes driven by active deformation (Pirmez et al.,  
45 2000; Ferry et al., 2005), individual case studies to-date show a wide range of channel  
46 responses to growing structure (Clark and Cartwright, 2009, 2012; Jolly et al., 2016; Mitchell  
47 et al., 2020). While theory and empirical observation suggest relationships between  
48 increased slope, structural uplift and channel incision/deflection, the sensitivity of submarine  
49 channels to the magnitude and rate of active deformation has never been comprehensively  
50 quantified (Clark and Cartwright, 2009, Mayall et al., 2010; Deptuck et al., 2012; Jolly et al.,  
51 2017; Mitchell et al., 2020). In particular, no study has attempted a robust statistical analysis  
52 of a large number of submarine channel-structure crossings in time and space, where  
53 deformation rates are measured independently. Here we address this challenge. We use 3D  
54 seismic reflection data on the southern lobe of the Niger Delta (Fig. 1), to determine the  
55 frequency distribution of Miocene to Pliocene channel systems where they cross gravity-  
56 driven fold-thrusts whose strain rate evolution is exceptionally well constrained (Pizzi, 2019;  
57 Pizzi et al., 2020). We quantify the strain rates where channels cross structures, compared to  
58 the fault array as a whole, throughout the 11 Myr growth history of the fold and thrust belt.  
59 For the first time, we test statistically the hypothesis that submarine channels are sensitive to  
60 on-going deformation near the seabed, and quantify when, where and with what probability  
61 submarine channels can cross active structures.

62

## 63 **STUDY AREA AND METHODS**

64 The Niger Delta (Fig. 1A) has an area of 140,000 km<sup>2</sup> with 12 km of sediments deposited  
65 since the Early Eocene (Damuth, 1994). The rapid advance of the delta above slope and pro-  
66 delta shale units facilitated the gravitational collapse of the system since the Miocene (e.g.  
67 Morgan, 2003; Bilotti and Shaw, 2005). The gravity failure was accommodated by

68 extensional tectonics on up-dip areas, and shortening towards the delta toe (Damuth, 1994;  
69 Fig. 1).

70

71 The study area is located on the lower slope of the delta (Fig. 1A) where numerous submarine  
72 channel systems have interacted with contractional structures from the Miocene to the present  
73 day (Fig. 1B) (Jolly et al., 2016, 2017; Mitchell et al., 2020). Using 3D seismic data, Pizzi  
74 (2019) and Pizzi et al. (2020) comprehensively quantified the structural evolution of eleven  
75 thrusts on the southern lobe of the Niger Delta (thrusts 12 to 22, Fig. 2A, B). The thrusts  
76 initiated at or before 15 Ma, with strain varying between structures and along strike, and also  
77 through time. Increases in fault length, associated with along-strike interaction and linkage,  
78 mostly occurred prior to 7.4 Ma. Deformation increased significantly between 9.5-6.5 Ma  
79 with shortening rates  $> 200$  m/My. We exploit the unique availability of detailed maps of  
80 strain rate evolution (Pizzi, 2019; Pizzi et al., 2020; *supplementary material*), such as the 5.5-  
81 3.7 Ma interval shown in Fig. 2C, as a well-constrained template of deformation rate and  
82 magnitude to test the sensitivity of submarine channels to active deformation.

83

84 Deep-water slope channels crossing coeval active fault segments were identified within six  
85 temporal intervals from 15 to 3.7 Ma (Pizzi et al., 2020; Table S1) using standard seismic  
86 stratigraphic techniques including multiple seismic sections and RMS amplitude extractions  
87 (*supplementary material*, Figs. S2-S5, Pizzi, 2019). For each interval, channel courses were  
88 overlain on the corresponding strain rate map, to record the fault strain rate at each channel-  
89 fault intersection, as shown in Figure 2C. This yielded 173 channel crossings between 15 and  
90 3.7 Ma, noting that a single channel may cross multiple structures (Fig. S6). Histograms were  
91 derived of (i) the strain rate recorded at channel crossings and (ii) the strain rate as a function  
92 of the total length of active fault segments, to capture the strain rate distribution for the  
93 overall fault array relative to the channel-fault intersections (Fig. 3A, B). The maximum  
94 length of all the faults in the array for any one time interval was 417 km. The mean strain rate  
95 for channel-fault intersections and the fault array at each time interval were recorded. The  
96 results for each unit were summed and normalized to derive three cumulative density  
97 functions as a function of strain rate; one of the number of channel crossings, and two  
98 depicting the cumulative distribution of fault segment lengths, with and without segments of  
99 zero strain, which were subsequently or previously active (Fig 3C). To test the hypothesis  
100 that the strain rates at submarine channel-fault crossings are significantly different from strain  
101 rates in the fault array, it must be demonstrated they are not drawn from the same underlying  
102 distribution, given we have not sampled all possible channels crossing faults on the southern  
103 lobe of the Niger Delta. We used a two sample Kolmogorov-Smirnov test (K-S test) to  
104 evaluate this. The null hypothesis - that the distribution of strain rates at channel crossings is  
105 the same as the distribution of fault segment strain rates - was tested at the 95% confidence  
106 interval (*supplementary material*, Tables S2, S3). We perform the K-S test for channel  
107 crossings at the scale of the whole fault array rather than on individual or groups of structures  
108 across strike to avoid arbitrary grouping of data that may pre-determine the results and to  
109 obtain statistically valid sample sizes.

110

## 111 RESULTS

112 We obtained a cumulative total of 2505 km of faults active in the period between 15 Ma to  
113 3.7 Ma (Fig. 3A; Table S3). All segments were active between 7.4 and 6.5 Ma; in the earlier  
114 and later intervals some were inactive (Pizzi et al., 2020, Fig. S6). Modal strain rates of 0 to  
115 1 %/My ( $\sim 70$  m/My) are documented for the thrusts, with a significant proportion at higher  
116 strain rates (Fig. 3A). A more conservative approach, excluding zero-strain rate segments for  
117 any time interval, yields 2139 km of active fault segments over the period. Presented as  
118 cumulative density functions (Fig. 3C), 50% of the fault segments were active at rates of  
119 more than 1.5 %/My in the period between 15 Ma and 3.7 Ma (red curve) or at more than 1.1  
120 %/My if zero strain rate segments are included (dashed red curve).

121

122 The channel-fault intersections as a function of strain rate (Fig. 3B) show a markedly  
123 different distribution. The modal number of channel crossings occurred for strain rates up to  
124 1%/My; an additional 48 crossings occurred over fault segments that were then inactive.  
125 However fewer crossings are recorded at higher strain rates. Only 4 channels cross structures  
126 with rates  $> 5\%/My$ , and none are documented for strain rates  $> 7\%/My$ . Significantly, the  
127 cumulative density function (Fig. 3C) shows that 50% of the crossings occurred for strain  
128 rates smaller than  $0.6\%/My$ , a value 2.5 times less than the median of the active fault  
129 segments ( $1.5\%/My$ ). Consequently, the distribution of channels is skewed towards smaller  
130 values of strain rate. A K-S test at the 95% confidence interval confirms we can reject the  
131 null hypothesis that the two observed distributions sample the same underlying distribution.  
132 Indeed, our results show that we can reject the null hypothesis at a higher 99.9% confidence  
133 interval (Table S3). Consequently, our data demonstrate unambiguously that submarine  
134 channels on a structured slope statistically exploit locations of lower strain rate to cross  
135 evolving faults over 11 My period, and enables us to quantify for the first time how this  
136 distribution differs from strain rates in a fault array as a whole.

137

138 Mean fault strain rate in each time interval increases until ca. 7 Ma, followed by decreasing  
139 strain rate thereafter (Fig. 4A). The faults deformed at an average rate of  $0.5\%/My$  from 15  
140 to 9.5 Ma, reached a peak of  $3.3\%/My$  ( $\sim 230$  m/My) in the 7.4 to 6.5 Ma interval, and  
141 decreased to ca.  $1.5\%/My$  by 4 Ma. Mean strain rates recorded at the channel crossings  
142 follow a similar pattern. However, while initially values were close to those for the whole  
143 fault array, they subsequently diverged when strain rates exceeded  $\sim 1\%/My$  threshold, with

144 channel crossings occurring at lower values of strain rate than the fault array mean. The  
145 number of channel crossings progressively decreased from 15 Ma to the 7.4-6.5 Ma interval  
146 and then increased thereafter (Fig. 4B). However, the trend is asymmetric such that a slow  
147 decrease in the number of channel crossings is followed by a marked increase when  
148 deformation slows after 6.5 Ma. Despite the reduction in shortening rate, the mean strain rate  
149 at channel crossings remains suppressed relative to that of the fault array for the youngest  
150 units 2 and 1 (Fig. 4A) showing a fast response of channel systems to changing boundary  
151 conditions, with new channels entering the area rapidly locating themselves so as to cross  
152 fault segments with lower strain rates.

153

## 154 **DISCUSSION**

155 Two-thirds of all channel-fault intersections over a period of ca. 11 Myr occurred at strain  
156 rates lower than 1%/My while the median strain rate of the array over the period was  
157 1.5%/My – a statistically significant difference (Fig. 3). While individual examples of  
158 channels crossing fast deforming faults can be found, our results are powerful because they  
159 quantify how the *probability* of channels crossing high strain rate structures reduces  
160 progressively as fault strain rates grow beyond 1%/My. We therefore caution against  
161 generalising models of channel behaviour from individual examples. The evolution of strain  
162 rates at the channel crossings mirrors, but is persistently lower than that of the fault array  
163 (Fig. 4A). Consequently, while submarine channel crossings are forced to follow the tectonic  
164 history of the area, the channels during each time interval actively locate to, or remained  
165 pinned at, points of lower strain rate to cross growing structures. We hypothesise that the  
166 control is structurally-mediated paleo-topography, the growth of which is enhanced by thrust  
167 fault linkage (see Pizzi et al., 2020). Although converting shortening rates into uplift rates  
168 requires assumptions (c.f Hardy and Poblet, 2005; Jolly et al., 2016; Mitchell et al., 2020),  
169 these shortening rates imply crestal uplift rates of equivalent magnitude for flexural-slip fault  
170 propagation folds, and have been shown to be sufficient to deflect sub-modern seabed  
171 channels on the Niger Delta (Jolly et al., 2017).

172

173 That the number of channel crossings decreases for greater values of strain rate and increases  
174 as soon as strain rates decrease (Fig.4B) reflects the reduced number of pathways that  
175 channels can realistically exploit to reach more distal areas during times of intense structural  
176 deformation and the potential for sediment ponding up-dip of structures (Clark and

177 Cartwright, 2012; Pizzi, 2019) (Fig. 2c; Fig. S4). Therefore, not only are channels deflected  
178 by deforming structures, even for relatively low strain rates, but the network is focused at a  
179 small number of crossing points when deformation rates are high (Fig 2c). However, when  
180 mean strain rates fall, new channels locate themselves rapidly at additional fault crossing  
181 points that still have lower-than-average deformation rates. Consequently, the locus and  
182 magnitude of sediment supply to deep water basins is predictably influenced by the 4D  
183 growth history of contractional faults on structured margins and the incompleteness of marine  
184 sedimentary records down-system of interacting faults will track the strain rate evolution of  
185 the array. The statistical distributions and methodology presented here could be used to  
186 predict submarine channel routing on structured slopes, even where seismic imaging is  
187 limited. Consequently, this type of analysis serves as a powerful tool to reconstruct sediment  
188 confinement and the routing of sands and pollutants to deep water.

189

## 190 **CONCLUSIONS**

191 From a statistical analysis of 173 submarine channel-fault crossings in the deep-water Niger  
192 Delta, and a cumulative 2505 km of fault segments for which strain rates have been  
193 calculated over an 11 Myr history, we show that:

194 1. Distributions of fault array strain rate and submarine channel-fault crossing strain rate are  
195 statistically different using a two-sample K-S test. The median strain rate where channels  
196 cross faults is  $< 0.6\%/Ma$ , 2.5 times lower than the median deformation rate of active fault  
197 segments ( $1.5\%/My$ ;  $\sim 100m/My$ );

198 2. Our results prove statistically that at a population level, channels exploit available  
199 locations of lower strain rate to cross active structures, although the mean strain rate at  
200 crossing points tracks the deformation history of the area; we hypothesise this control is  
201 exerted by fault-induced topography on the sea-bed.

202 3. The submarine channel network focusses into fewer channels crossing faults at higher  
203 strain rates. However as soon as the deformation rates decrease, submarine channels rapidly  
204 locate themselves in areas of relatively lower strain rate.

205 4. Our results caution against the use of individual channel examples to deduce submarine  
206 channel sensitivity to active deformation; illustrate how population statistics give rise to a  
207 step-change in our understanding of typical submarine channel behaviour; and demonstrate  
208 that strain rate analyses are a powerful tool for predicting the routing of sands and pollutants  
209 to deep water.

210



211 **ACKNOWLEDGEMENTS**

212 MP was funded by the NERC CDT in Oil & Gas. Data was provided by PGS and the  
213 Nigerian Petroleum Directorate. We thank E. Taylor and R. Lamb for data access and  
214 acknowledge software donations from Landmark-Halliburton and StructureSolver <sup>TM</sup>. We  
215 thank Tim Cullen and two anonymous reviewers for their constructive comments.

216

217 **FIGURE CAPTIONS**

218 Figure 1: – A) Location and setting of the Niger Delta. Study area shown as orange box. B)  
219 Three-dimensional image from the south of the study area showing submarine channels  
220 (dashed white lines) interacting with folds (black dashed lines) of the outer fold-and-thrust  
221 belt. Study interval of ~15-3.7 Ma highlighted in yellow.

222

223 Figure 2 A) Depth-structure map of the 9.5 Ma horizon showing eleven thrusts, labelled 12-  
224 22, deforming the lower slope. B) Cross-section through the seismic data showing folds and  
225 mapped horizons, adapted from Pizzi et al., (2020). Fig. S2 shows the uninterpreted seismic  
226 section. C) Example strain rate map for the 5.5-3.7 Ma interval, showing spatial variation in  
227 fault segment strain rate. Strain was calculated using a normalised line length of 7 km.  
228 Submarine channel systems were mapped and their crossing locations and associated strain  
229 rate (circles) were recorded (see Supplementary material).

230

231 Figure 3: Histograms of: (A) Total kilometres of active fault segments and (B) Total number  
232 of channel-fault crossings against strain rate over 11 Myr fault array history. (C) Cumulative  
233 density functions from the histograms above for the strain rate of active faults (red line),  
234 those including segments of zero strain (red dashed line); and strain rate of channel-fault  
235 crossings. 50% of channels exploited strain rates <0.6%/Ma, while 50% of faults deformed at  
236 rates above 1.5%/Ma.

237

238 Figure 4: (A) Mean shortening and strain rates against time for the fault array as a whole and  
239 for channel-fault crossings. (B) Number of channel crossings and strain rate for the fault  
240 array as a whole against time. Number of channel crossings at 5.5 Ma is a minimum estimate  
241 as some poorly imaged channels are not included.

242

243

244 **REFERENCES CITED**

- 245 Babonneau, N., Savoye, B., Cremer, M., and Klein, B. 2002, Morphology and architecture of  
246 the present canyon and channel system of the Zaire deep-sea fan. *Marine and Petroleum*  
247 *Geology*, v. 19(4), p. 445-467.
- 248 Bourget, J., Zaragosi, S., Ellouz-zimmermann, N., Mouchot, N., Garlan, T., Schneider, J. L.,  
249 and Lallemand, S. 2011, Turbidite system architecture and sedimentary processes along  
250 topographically complex slopes: the Makran convergent margin. *Sedimentology*, v.  
251 58(2), p. 376-406.
- 252 Bilotti, F. and Shaw, J.H., 2005, Deep-water Niger Delta fold and thrust belt modeled as a  
253 critical-taper wedge: The influence of elevated basal fluid pressure on structural styles.  
254 *AAPG Bulletin*, v. 89(11), p.1475-1491.
- 255 Callec, Y., Deville, E., Desaubliaux, G., Griboulard, R., Huyghe, P., Mascle, A., and  
256 Schmitz, J. 2010, The Orinoco turbidite system: Tectonic controls on sea-floor  
257 morphology and sedimentation. *AAPG bulletin*, v. 94(6), p. 869-887.
- 258 Corredor, F., Shaw, J.H. and Bilotti, F., 2005, Structural styles in the deep-water fold and  
259 thrust belts of the Niger Delta. *AAPG Bulletin*, v. 89(6), p. 753-780.
- 260 Covault, J. A., Sylvester, Z., Hubbard, S. M., Jobe, Z. R., and Sech, R. P., 2016, The  
261 stratigraphic record of submarine-channel evolution: *The Sedimentary Record*, v. 14, p.  
262 4-11.
- 263 Clark, I. R., and Cartwright, J. A. 2009, Interactions between submarine channel systems and  
264 deformation in deepwater fold belts: Examples from the Levant Basin, Eastern  
265 Mediterranean sea. *Marine and Petroleum Geology*, v. 26(8), p. 1465-1482.
- 266 Clark, I. and J. Cartwright, 2012, Interactions between coeval sedimentation and deformation  
267 from the Niger Delta deepwater fold belt, *SEPM Special Publication 99*, p.243-267.
- 268 Damuth, J., 1994, Neogene gravity tectonics and depositional processes on the deep Niger  
269 Delta continental margin, *Marine and Petroleum Geology*, v. 11, p.320-346.
- 270 Deptuck, M. E., Sylvester, Z., and O'Byrne, C. 2012, Pleistocene seascape evolution above a  
271 "simple" stepped slope, western Niger Delta. Application of the principles of seismic  
272 geomorphology to continental slope and base-of-slope systems: Case studies from sea  
273 floor and near-sea floor analog: *SEPM Special Publication 99*, p. 199-222.
- 274 Don, J., Shaw, J. H., Plesch, A., Bridgwater, D. D., and Lufadeju, G. 2019, Characterizing the  
275 growth of structures in three dimensions using patterns of deep-water fan and channel  
276 systems. *AAPG Bulletin*, v. 104 (1), p. 177-203.

277 Ferry, J. N., Mulder, T., Parize, O., & Raillard, S. 2005, Concept of equilibrium profile in  
278 deep-water turbidite system: effects of local physiographic changes on the nature of  
279 sedimentary process and the geometries of deposits. Geological Society of London  
280 Special Publication, 244(1), p. 181-193.

281 Hardy, S., and Poblet, J. 2005, A method for relating fault geometry, slip rate and uplift data  
282 above fault-propagation folds. Basin Research, v. 17(3), p. 417-424.

283 Howlett, D. M., Ge, Z., Nemec, W., Gawthorpe, R. L., Rotevatn, A., and Jackson, C. A. L.  
284 2019, Response of unconfined turbidity current to deep-water fold and thrust belt  
285 topography: Orthogonal incidence on solitary and segmented folds. Sedimentology, v.  
286 66(6), p. 2425-2454.

287 Jolly, B.A., Lonergan, L. and Whittaker, A.C., 2016, Growth history of fault-related folds and  
288 interaction with seabed channels in the toe-thrust region of the deep-water Niger delta.  
289 Marine and Petroleum Geology, v. 70, p. 58-76.

290 Jolly, B.A., Whittaker, A.C. and Lonergan, L., 2017, Quantifying the geomorphic response of  
291 modern submarine channels to actively growing folds and thrusts, deep-water Niger  
292 Delta. Geological Society of America Bulletin, v. 129, p. 1123-1139.

293 Kane, I. A., and Clare, M.A., 2019, Dispersion, Accumulation, and the Ultimate Fate of  
294 Microplastics in Deep-Marine Environments: A Review and Future Directions, Frontiers  
295 in Earth Sciences, v. 7, A80, doi.org/10.3389/feart.2019.00080.

296 Mayall, M., Jones, E., and Casey, M. 2006, Turbidite channel reservoirs—Key elements in  
297 facies prediction and effective development. Marine and Petroleum Geology, v. 23(8), p.  
298 821-841.

299 Mayall, M., Lonergan, L., Bowman, A., James, S., Mills, K., Primmer, T., and Skeene, R.  
300 2010, The response of turbidite slope channels to growth-induced seabed topography.  
301 AAPG bulletin, v. 94(7), p. 1011-1030.

302 Mitchell, W. H., Whittaker, A., Mayall, M., Lonergan, L., and Pizzi, M., 2020, Quantifying  
303 the relationship between structural deformation and the morphology of submarine  
304 channels on the Niger Delta continental slope, Basin Research,  
305 doi.org/10.1111/bre.12460 (in press).

306 Morgan, R., 2003, Prospectivity in ultradeep water: the case for petroleum generation and  
307 migration within the outer parts of the Niger Delta apron. Geological Society of London,  
308 Special Publication, 207, p.151-164.

309 Pirmez, C., Beaubouef, R. T., Friedmann, S. J., Mohrig, D. C., and Weimer, P. 2000,  
310 Equilibrium profile and baselevel in submarine channels: examples from Late

311 Pleistocene systems and implications for the architecture of deepwater reservoirs. In  
312 Global deep-water reservoirs: Gulf Coast Section SEPM Foundation 20th Annual Bob F.  
313 Perkins Research Conference, p. 782-805. ISBN: 9781605603322.

314 Pizzi, M. 2019. Quantification of tectonic controls on the distribution and architecture of  
315 deep-water facies during the growth of the toe-thrusts region of the Niger Delta, PhD  
316 thesis, Imperial College London, 238 pp. doi.org/10.25560/85679.

317 Pizzi, M., Lonergan, L., Whittaker, A.C., and Mayall, M., 2020, Growth of a thrust fault  
318 array in space and time: An example from the deep-water Niger delta: *Journal of*  
319 *Structural Geology*, v. 137, 104088, 10.1016/j.jsg.2020.104088.

320 Sømme, T. O., Helland-Hansen, W., Martinsen, O. J., and Thurmond, J. B. 2009,  
321 Relationships between morphological and sedimentological parameters in source-to-sink  
322 systems: a basis for predicting semi-quantitative characteristics in subsurface systems.  
323 *Basin Research*, v. 21(4), p. 361-387.

324 Smith, R. U. 2004, Silled sub-basins to connected tortuous corridors: Sediment distribution  
325 systems on topographically complex sub-aqueous slopes. Geological Society of London,  
326 Special Publication 222, p. 23-43.

327 Sweet, M. L., and Blum, M. D., 2016, Connections between fluvial to shallow marine  
328 environments and submarine canyons: Implications for sediment transfer to deep water.  
329 *Journal of Sedimentary Research*, v. 86(10), p. 1147-1162.

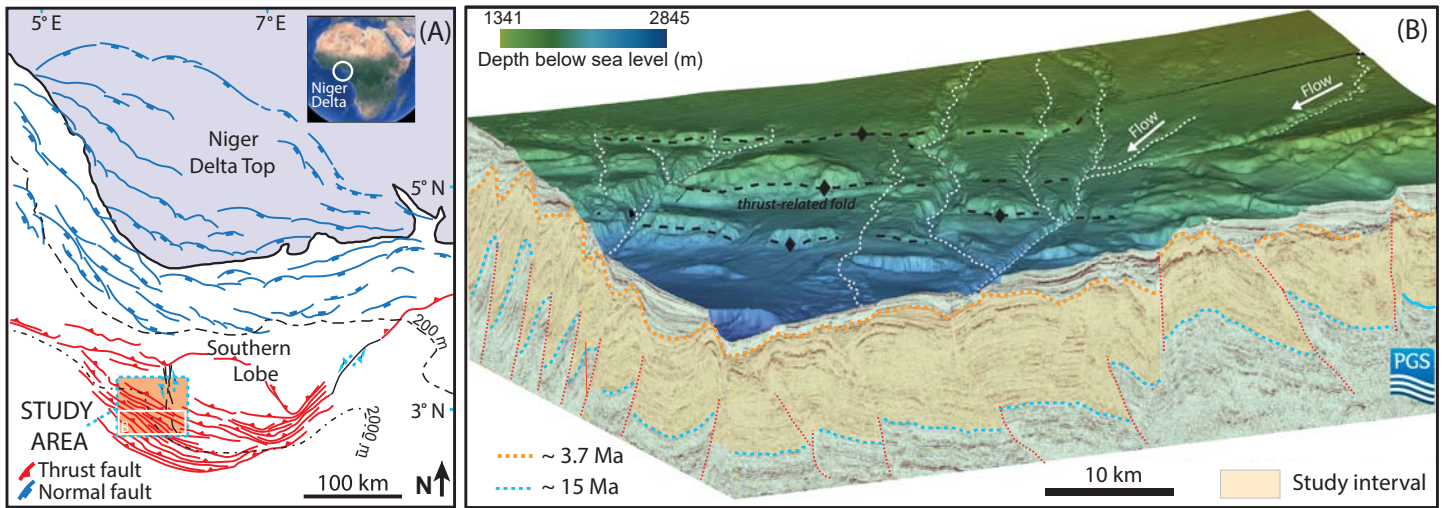
330 Talling, P., J. Allin, D.A. Armitage, R.W.C. Arnott, M.J.B. Cartigny, M.A. Clare, F. Felletti,  
331 J.A. Covault, S. Girardclos, E. Hansen, P.R. Hill, R.N. Hiscott, A.J. Hogg, J. Hughes  
332 Clarke, Z.R. Jobe, G. Malgesini, A. Mozzato, H. Naruse, S. Parkinson, F.J. Peel, D.J.W.  
333 Piper, E. Pop, G. Postma, P. Rowley, A. Sguazzini, C.J. Stevenson, E.J. Sumner, Z.  
334 Sylvester, C. Watts, J. Xu, 2015, Key future directions for research on turbidity currents  
335 and their deposits: *Journal Sedimentary Research*, v. 85, p. 153-169.

336

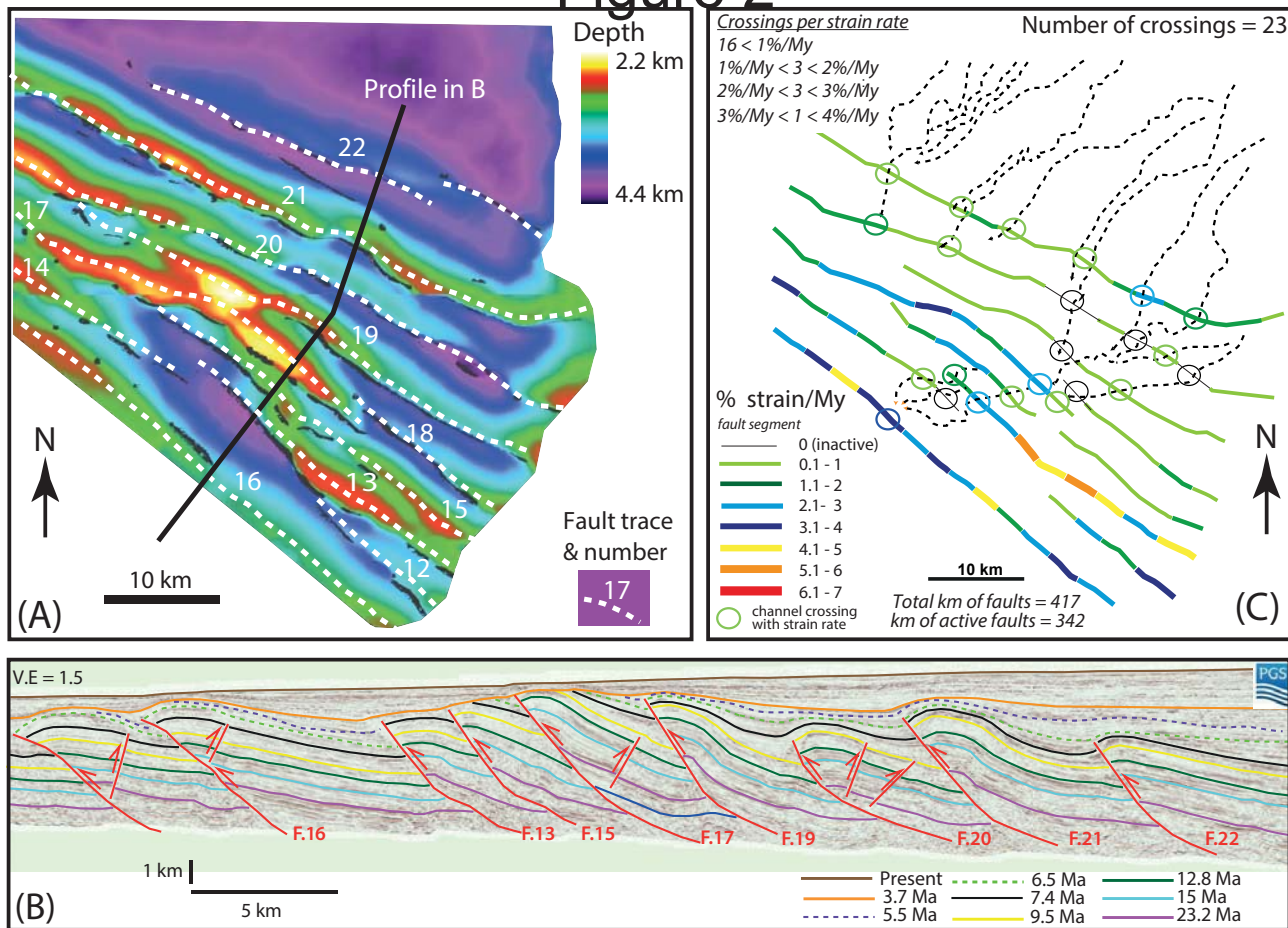
337

Figure 1

FIGURE 1



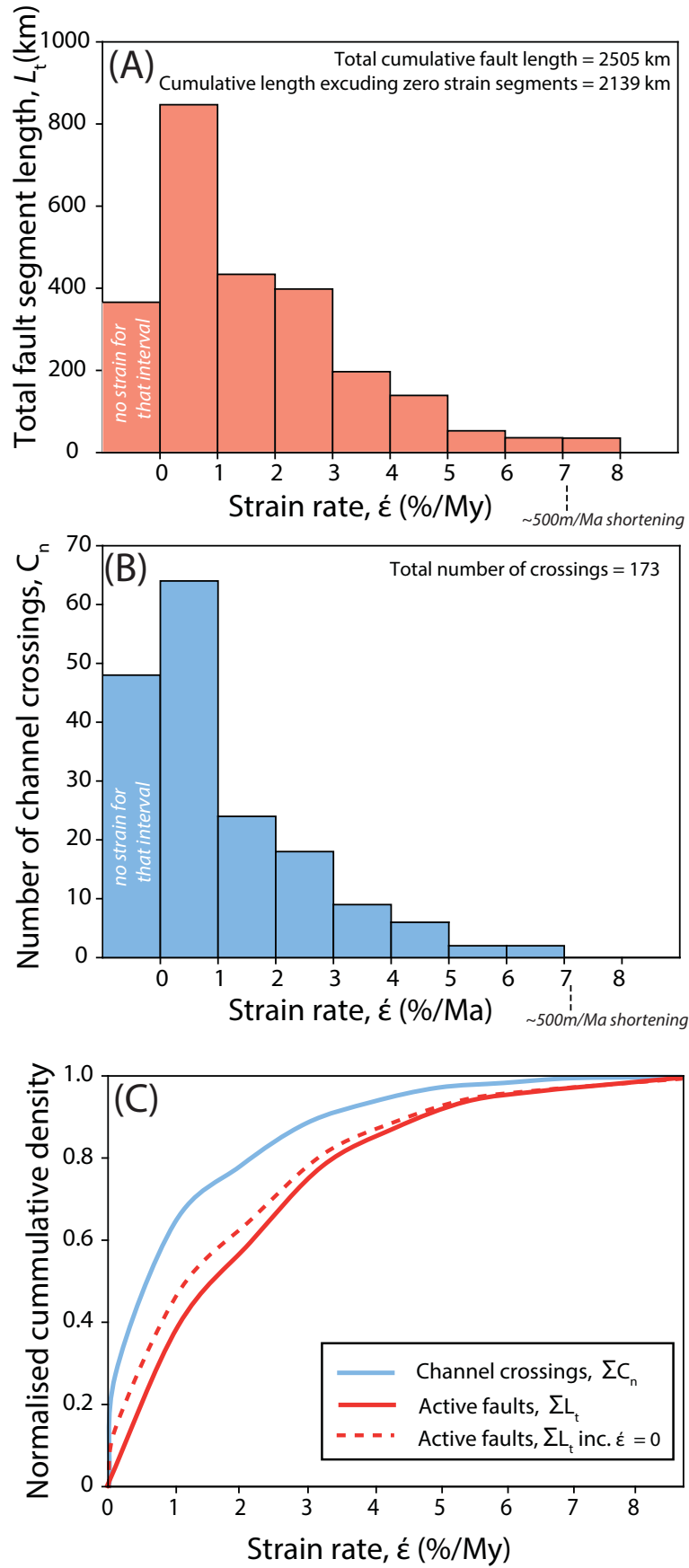
# Figure 2



## Figure 2

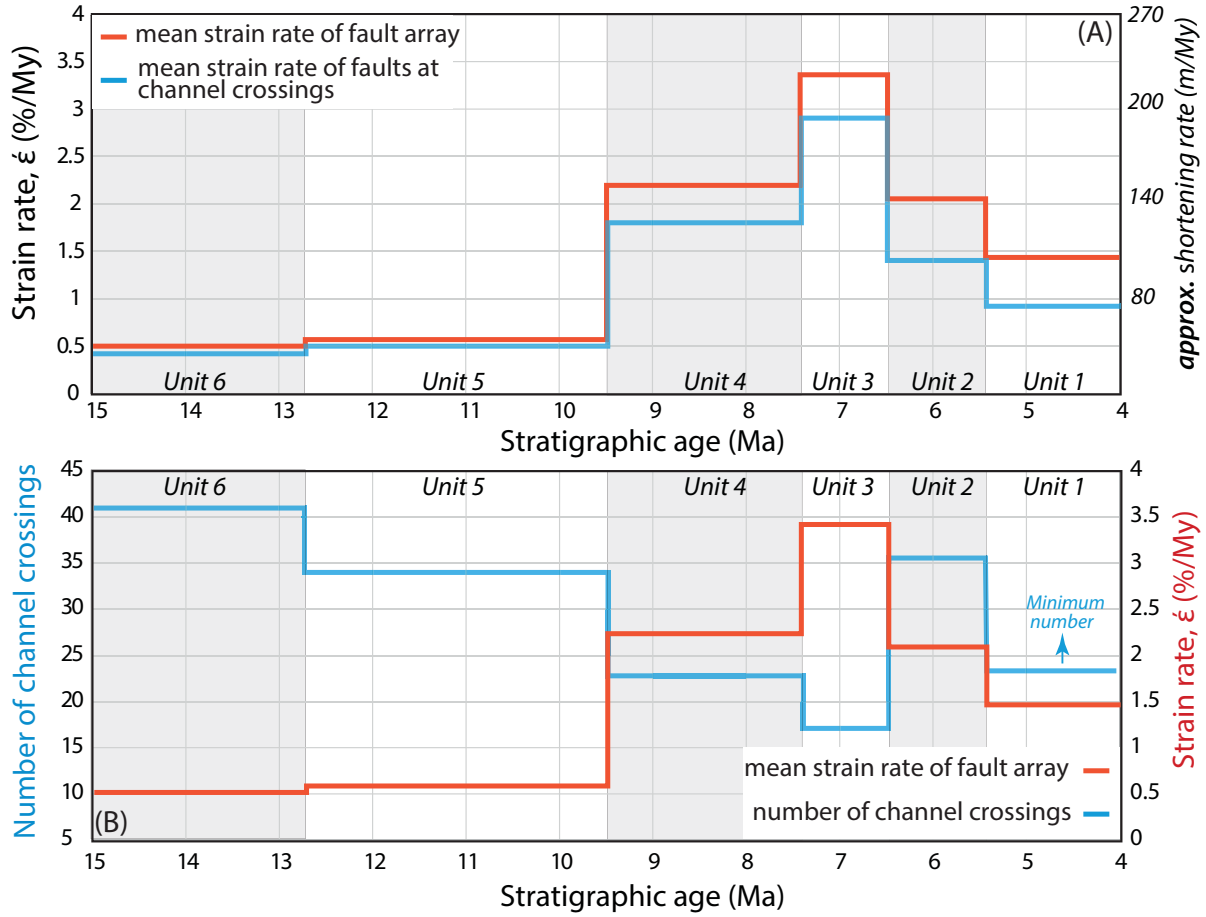
# Figure 3

Figure 3



# Figure 4

Figure 4





**Dr Alexander Whittaker**

Senior Lecturer (Associate Professor) in Tectonics  
a.whittaker@imperial.ac.uk  
[www.imperial.ac.uk/people/a.whittaker](http://www.imperial.ac.uk/people/a.whittaker)

Monday, February 15, 2021

Manuscript G48698 'New statistical quantification of the impact of active deformation on the distribution of submarine channels'.

Dear Prof. Dickens

We were delighted to see that our manuscript received a positive response from all three reviewers. We have been through the reviewers' comments carefully and have addressed all of their comments. These are laid out comprehensively in the point-by-point comments, below. You asked us to ensure that 1) the impact of the work was elevated and made clear to readers; and (2) to ensure more detail about channel imaging and background was included in the supplementary material, notwithstanding that this should not include lots of additional material that requires further review.

We have taken both of these two points seriously and have addressed them directly (Editor Comments, below). We have re-edited the main text of the manuscript to make sure the novelty of this exciting work is as clear as possible to readers. We have also added some additional figures and ancillary text into the supplementary material, as you suggested, and we have ensured with Library Services at Imperial College that the PhD thesis of Pizzi, which contains an abundant description of the seismic data is publically available to download on the official college library website with its own doi. This means that all the background data is available to readers.

All our changes are tracked in Word – line numbers refer to the 'unmarked-up' version of the new manuscript. We are very grateful for the constructive comments from the reviewers and from you, and we trust the manuscript is now ready for publication in Geology.

Yours sincerely,



Dr Alexander Whittaker

## **Editor Comments:**

1/ Elevate the impact of the work. Good GEOLOGY papers should be provocative, but referees clearly point out that the results are in some way almost self-evident.

It was great to read that the reviewers really supported the science and the results. It is exciting work! We agree with the reviewers that we underplayed the importance of our findings. This was out of genuine desire not to be guilty of ‘over-hyping’ the results but we accept we should stress the impact for the readers more. **Our results are the first time the sensitivity of submarine channels to growing structure has ever been demonstrated statistically at a population level.** The sensitivity is not binary – the point is that the statistical distributions quantify how submarine channels are *increasingly likely* to be defeated by high-slip rate faults. The power in this analysis is that we can use these distributions to predict the probability of channels crossing growing structures, as well as their location, to determine sediment and pollutant routing to deep water. **None of this has ever been done before.**

Case studies describing a wide range of individual channel interactions in a qualitative way are often published in regional journals. Our results challenge this type of descriptive approach and show real insights and predictive power come from quantifying at the statistics of large numbers of channels. This is because even in a population set like this you can find examples of e.g. a channel cutting across a high strain rate structure. Our results therefore caution against generalising from individual examples – which unfortunately is what is typically published in this field. To make the novelty and impact super clear for readers, we have revised the abstract, intro, discussion and conclusions carefully to stress why the work matters so much:

The abstract now points out (L26) “*Our results quantify the sensitivity of submarine channels to active deformation at a population level for the first time, and enable us to predict the temporal and spatial routing and distribution of submarine channels affected by structurally-driven topography*”

In the intro we highlight that (L43) “*Although it is often assumed that submarine channels are sensitive to topographic changes driven by active deformation (Pirmez et al., 2000; Ferry et al., 2005), individual case studies to-date show a wide range of channel responses to growing structure (Clark and Cartwright, 2009, 2012; Jolly et al., 2016; Mitchell et al., 2020).*”

We add that (L48) “*...the sensitivity of submarine channels to the magnitude and rate of active deformation has never been comprehensively quantified (Clark and Cartwright, 2009, Mayall et al., 2010; Deptuck et al., 2012; Jolly et al., 2017; Mitchell et al., 2020). In particular, no study has attempted a robust statistical analysis of a large number of submarine channel-structure crossings in time and space, where deformation rates are measured independently. Here we address this challenge.*”

The novelty is restated at the end of the intro (L58) “*For the first time, we test statistically the hypothesis that submarine channels are sensitive to on-going deformation near the seabed, and quantify when, where and with what probability submarine channels can cross active structures.*”

In the discussion we now state explicitly that (L155) “*While individual examples of channels crossing fast deforming faults can be found, our results are powerful because they quantify how the probability of channels crossing high strain rate structures reduces progressively as fault strain rates grow beyond 1%/Ma. We therefore caution against generalising models of channel behaviour from individual examples.*”

We also stress the predictive power of the results, which reviewer 3 raises too (L182) “*The statistical distributions and methodology presented here could be used to predict submarine channel routing on structured slopes, even where seismic imaging is limited. Consequently, this type of analysis serves as a powerful tool to reconstruct sediment confinement and the routing of sands and pollutants to deep water.*”

In addition we have edited all the conclusions to make them, snappier, clearer and more impactful. There are number of smaller text edits throughout to stress the importance and reach of the work. We think the impact, significance and novelty of this exciting work is now clear for readers of Geology.

2/ Add additional data to the Supplementary Information. This is somewhat tricky, because it should NOT include lengthy text or interpretations that require review. Moreover, it should NOT be data or figures that you may want to publish elsewhere. Rather, this might be a few additional figures that bolster the science.

All three reviewers suggest some additional supplementary information about the method and channel interpretation. We are happy to do this. We have added a line to the main text of the manuscript (L85) stating explicitly how we have mapped the channels. We have added more detail to the supplementary material explaining the channel mapping and imaging. In particular, we have revised Fig. S2 to zoom in on one of the intervals with an improved reversed colour scheme so readers get a better idea of what we looked at. We have provided two additional figures (Fig. S4, S5) that illustrate the presence and characteristics of the channels. These are adapted from the PhD thesis of Pizzi (2019).

However - we note seriously your caveat as Editor about how much detail to provide. Fundamentally, this paper is a statistical evaluation of the frequency of nearly 200 seismically-mapped submarine channel crossings of faults as a function of strain rate, compared to a fault array as a whole. The paper is not actually about the details of submarine channel imaging, nor the mechanics of strain evolution in fault arrays.

- 1) For the channel imaging and channel crossings - these come from a detailed examination of a 3D seismic volume of a portion of the Niger Delta, including RMS amplitude extractions and many seismic sections. These methods and accompanying data are described in Pizzi's extensive PhD thesis (2019), examined and fully corrected by Peter Haughton and Gary Hampson. **We have ensured that it is now open access from Imperial College London and it has its own doi: [doi.org/10.25560/85679](https://doi.org/10.25560/85679). It is available to download from the official college library website: <https://spiral.imperial.ac.uk/handle/10044/1/85679>.** This directly answers reviewer 3's comments about the availability of this background work. We think it is reasonable to direct readers to this publicly-available thesis for a detailed description of the seismic data. However we agree we can provide more detail on the *types of method* used to map the channels, consistent with other studies, and we have provided more background in section 3 of the supplementary material. However, it would be impossible to publish any statistical study of this type if it were intended that each of the ca. 200 channel crossings should be presented and analysed in detail in the manuscript.
- 2) The fault array evolution has been fully published in the *Journal of Structural Geology* (Pizzi et al., 2020). Questions about the methods of calculating strain rate, fault displacement etc are fully answered in this study so we think it is reasonable to direct readers and reviewers to this if they want more detail. Reviewer 2 had some detailed comments about e.g. the distribution of lobes, channel responses to along strike variation in strain etc. They also ask about the mechanisms of channel relocation. These are interesting questions and we have provided some clarification for this where possible (see below) - but many of these points are properly topics for a separate paper, which we are currently writing.

We trust this strikes the right balance between helping the reader but not overloading the supplementary material with extraneous detail freely available elsewhere, or with material that needs further review.

**Reviewer #1 (Comments to the Author):**

This manuscript describes the interaction of submarine slope channels with faults in the deep-water Niger Delta and shows that the median strain rate where channels cross faults is significantly lower than the median strain rate of active fault segments. This is not an unexpected result, but the contribution is novel in the sense that it quantifies the strain rates along the faults and maps a relatively large number of channels that cross the faults, creating the possibility for a statistical analysis. The paper is well written, quite nicely illustrated, and well-focused, and it will clearly add to our knowledge of how submarine channels interact with faults on the seafloor. We are extremely grateful for the reviewer's supportive comments and to read that they support publication. We are delighted that they think it is novel and adds to our knowledge of submarine channels. But we respectfully disagree with the assertion that our results might be considered as 'not unexpected'. Lots

of people have said submarine channels might be diverted or deflected around growing structures depending on circumstance. No-one to our knowledge has ever statistically quantified this assertion. The reviewer's expectation is presumably based on personal experience and observations. That is fine, but is always possible to find individual examples of channels displaying every type of behaviour from crossing a structure to being diverted or deflected. Only a statistical analysis can demonstrate typical behaviours at a population level! We accept that we should have been more explicit about why our results matter so much. To stress the importance of what we have done we have rewritten parts of the introduction, discussion and conclusion to make the impact of this work explicit for readers – this is laid out in the editor's comment 1, above.

1. This might be just a figure quality issue, but it is unclear to me how reliable are the channel maps when it comes to determining whether there is a channel crossing at a fault location. Example amplitude extractions are provided in Figures S2 and S3 of the Supplementary Material. Many mapped channels stop at the fault location and they are not mapped on the other side. What happens with these channels? Do they terminate in lobes? Are they being eroded? Or is it simply impossible to map the continuation on the other side of the fault, due to seismic quality issues? In addition, it is difficult to see in Figure S2 how the channels crossing faults 18, 19, and 20 were mapped as I cannot see any of them in the amplitude extractions. This is a figure quality issue which we have rectified (below) but also reflects the fact that channels and crossings have been identified from both RMS maps and multiple seismic sections taken from the 3D seismic volume.. We take the point about figure quality and we have formatted Figures S2 and S3 to show how we have used the RMS amplitude extractions- it is a larger, higher resolution image to illustrate the existence of channels crossing faults. Two more example figures (Figs S4, S5) have been inserted in the supplementary material from Pizzi, (2019) to demonstrate the imaging and nature of the channels. The 173 channel crossings were mapped based on a detailed examination of the seismic data, multiple sections, amplitude analyses etc, many of which are presented in the PhD thesis of Pizzi. We are confident that we have used a rigorous and repeatable process to map these channels. Rather than showing imaging of every crossing in the supplement, which would make it enormous, we follow the approach of other authors in describing the types of approach used, with appropriate examples. Section 3 of the supplementary text now provides further detail including any imaging issues encountered. Pizzi, 2019, which is available online to download, includes the full set of maps used for the interpretation and other background information. Where appropriate, we direct the reader to this.

2. The discussion of how channels establish new crossing points or abandon old ones is not very clear. For example, when the authors say that "new channels rapidly locate themselves at additional fault crossings with lower strain/shortening rates" (lines 180-183), it is unclear how this 'relocation' happens. Does it happen through ... avulsions, re-channelization, and knickpoint migration? We have edited the main text (L161) to say that *"Consequently, while submarine channel crossings are forced to follow the tectonic history of the area, the channels during each time interval actively locate to, or remained pinned at, points of lower strain rate to cross growing structures. We hypothesise that the control is structurally-mediated paleo-topography, the growth of which is enhanced by thrust fault linkage."* The detailed mechanisms, including avulsion and incision are interesting and we are writing a paper on this right now. But there is no room in a short geology paper to explore this ancillary topic. We would clearly need to present more figures and sections to illustrate these processes and they would not change the main paper findings.

3. The main conclusion of the paper is that channels preferentially cross faults where the strain rate is lower. This is not surprising; and I am wondering if there is a better way to argue that the results and methodology of this study can be used in places where the available data does not allow the mapping of channels. We agree – we should stress the novelty! Amongst other changes, we now explicitly state (L183) *The statistical distributions and methodology presented here could be used to predict submarine channel routing on structured slopes, even where seismic imaging is limited"*. We have also comprehensively re-edited our conclusions: Point 4 includes *"Our results caution against the use of individual channel examples to deduce submarine channel sensitivity to active deformation; illustrate how population statistics give rise to a step-change in our understanding of typical submarine channel behaviour; and demonstrate that strain rate analyses are a powerful tool for predicting the routing of sands and pollutants to deep water"* ( L203)

A couple of less important points: 1) It is unusual to use two significance levels (0.05 and 0.001) for a statistical test. If the hypothesis is rejected at the 0.001 level, it will obviously be rejected at the 0.05 level as well. A standard approach in the Earth sciences for deciding whether distributions are similar or not is whether the two-parameter K-S test can be accepted or rejected at the 95% confidence interval. We have included this accordingly, while noting that we can also reject the hypothesis of a similar distribution at a significance level of 0.001. We now clarify in the supplementary information that “*The null hypothesis (i.e. that the distribution of strain rates at channel crossing points is the same as the distribution of fault segment strain rates) was tested at the 95% confidence interval as a standard measure of whether the distributions were different. We also tested the null hypothesis at the 99.9% confidence interval as a rigorous upper limit*”.

2. Is it possible to change the colormap for Figure 2A, preferably to a perceptually monotonic one? We explored this for Fig 2A but if the depths are in black and white it is very difficult to see the faults and the section line, whatever shade of grey they are. However we have adapted Figure 2B in line with the comments of reviewer 3.

## **Reviewer #2**

This article explores how sea floor deformation controls the routing of deep-water channels using a 3D seismic dataset ... what is novel here is a detailed kinematic and strain characterisation of an evolving set of compressional fold-thrust structures (already published) combined with mapping of deep-water channels crossing these structures. A strength of the study is the statistical analysis of strain rates across the fold-thrust array as whole compared to rates occurring at channel crossing points and the demonstration that the distributions are different. *Thanks for the supportive comments!*

(1) Spatial variation in strain rate in dip direction: What is the impact of cross (as opposed to along) strike variations in strain rate on the statistical analysis given that all the active fold-thrust structures are considered together for each time interval, irrespective of location in the array? The study sets itself up as emphasising along-strike strain variation and refers to channels being directed to, or exploiting, lower strain segments 'along the strike of the faults'. However, the fold-thrust array shows significant cross strike variations with the time slice in Fig. 2C showing low strain on the up-dip structures and the more active structures located further down slope [... ] The issue is whether the statistics are bundling together instances in which channels are exploiting low strain sectors on actively growing structures having been directed there, but also channels merely draining across the first structures they encounter and which they have managed to bury.... One could envisage very different channel-crossing statistics in the instances where deformation and topography is focussed on up-dip structures vs. those where the more active structures are down dip. *This is an interesting question. We show several examples in the text and supplementary material where up-dip structures have higher strain rate than the down dip ones and this is true for most of the fold belt evolution. Channels cross structures at variable locations through time and while this could appear random, we demonstrate it is not by rejecting the null hypothesis using our K-S test approach. This is also illustrated in figure 4A which shows that the mean strain rate at channel crossing is lower than of the fault array, even at times of widespread low strain rates (e.g. Unit 6 and 5). The most evident impact of the across strike strain variations is shown by how widespread the channels are with low strain rates, and how focused they become in high-strain-rate regions. The robustness of a K-S test depends explicitly on the numbers of data points used and we achieve a statistically meaningful result at the scale of the fault array over the 6 time intervals without any imposed 'grouping' or selection of data. Although we could potentially sub-group the channel crossing data for different time intervals with different cross strike variations in strain in any number of combinations this raises the problems that (1) the number of crossings will be too small in some sub-groups to be statistically meaningful; and (2) a reviewer might fairly criticise us for an arbitrary division of the data that may pre-determine the outcome. We believe it is far more robust to present the data at the scale of the fault array without making choices about how to pre-package our channel crossings. To clarify this we have added the following to methods section of the main text (L106) “*We perform the K-S test for channel crossings at the**

*scale of the whole fault array rather than on individual or groups of structures across strike to avoid arbitrary grouping of data that may pre-determine the results and to obtain a statistically valid sample sizes.”*

The reviewer is right that there is additional detail in terms of along strike variations that could be explored. Further discussion and illustration of the impact of the along and across-strike strain variations (e.g. up-dip diversions due to up dip structures; facies and style of sedimentation etc) is present in chapter 7 of the Pizzi (2019) thesis. However these details do not change the headline results of this paper and are not required for this manuscript. Exploring this topic requires a bunch of other figures, analyses and discussion and is the subject of a forthcoming paper from our group.

(2) Channel imaging: The paper should say a little more on the channel imaging and perhaps provide an example in the body of the paper. Several crossings are shown (Fig. 2C) with no channel emerging down slope from them - did they cross? It is not clear why the channels are shown within the array in Fig. 2C are shown with a brown dashed line - is this significant? The caption to Fig. 4 mentions some crossings are not included for 5.5 Ma (presumably for unit 1 between 5.5 -3.7 Ma, although the axes of the graph is truncated at 4 Ma) as 'some poorly imaged channels' are not included. Is this a widespread issue? This same unit is shown in Fig. 2 to illustrate crossings - where are the poorly imaged channels? In higher strain areas there has been significant uplift and erosion - is it possible some channel crossings are missing in these areas because they have been removed and how significant an issue is this? We are happy to provide some more detail about channel imaging. We now clarify in the main text (L86) that channels have been identified “*using seismic stratigraphic techniques including multiple seismic sections and RMS amplitude extractions (supplementary material, Figs. S2, S3, Pizzi, 2019)*”. In the supplementary material we have added: (1) More ancillary text and two further figures adapted from Pizzi (2019) (Fig. S4 and S5) to show more examples of the channels identified and detail how channels were mapped and the imaging issues encountered. Different colours represent variable facies architectures; this is now described in the supplement and readers are referred to the PhD thesis of Pizzi, (2019) which include the full set of maps used for the interpretation and complete details. (2) a modified and focused version of Fig. S2 for the 5.5 to 3.7 Ma interval (unit 1) that clearly shows where and why some channels could not be mapped. This was a local issue in the centre of the fold belt at the later time slices where the more recent stratigraphy has been eroded. We compiled data across multiple time slices and conducted a formal K-S test precisely because we had not captured all possible channels - this is the point of the methodology we use. With the frequency of data we do have, it shows that even with the crossings we identified we can confidently reject the null hypothesis that channel crossings are insensitive to structure.

(3) External/wider controls: The number of crossings has been documented for the different units and linked to the changing strain rate. Fewer channel crossings at high strain rates are related to focussing of flow into a reduced number of pathways. Is it also possible there are longer term changes imposed by factors outside of the fold-thrust belt? For example, coeval up-dip extension during times of higher compressional strain rate may have opened up more accommodation higher on the slope, reducing flow frequency and channel activity downslope. Yes - it is certainly possible to hypothesise other longer term controls such as sediment delivery to the Niger Delta, which may have some influence on channel behaviour. But the key point is that over the course of the study (> 10 My) where channels cross faults is at a statistically significant lower strain rate than that of the fault array as a whole. This primary conclusion would be unaffected by these other controls. As the relationship between structure and channel routing is unequivocal in the Niger Delta (c.f. Jolly et al., 2016; Mitchell et al., 2020) we prefer to focus on this in the Geology paper rather than speculating on additional factors that are not fully constrained. We have a paper we are writing at the moment that focuses further on channel behaviour at a more detailed level so please watch this space!

The lobate bodies shown in Figure S4 should be keyed. What is the significance of the different coloured channels? The lobate bodies and the different coloured channels represent variable facies architectures (e.g. lobes, leveed and erosional channels etc.) which we now have keyed in the supplementary material. They are fully described in chapter 4 of the PhD thesis (Pizzi, 2019) and discussed in chapters 5 and 6 of this document;

we explicitly direct the reader to the thesis if they wish to know more. An analysis of the lobes is clearly outside of the scope of this manuscript, which is uniquely focused on the location and distribution of submarine channels.

**Reviewer #3 (Tim Cullen):**

Firstly, great work - this is a really nice and neat example of the value of quantifying these tectono-sedimentary relationships, and you've explained it really well. I remember seeing this presented at BSRG a couple of years ago so it is nice to see this being considered for publication as its a really neat story Thanks! Tim kindly produced a separate pdf review that provided several points to think about. We are really grateful for this. He also gave an email summary of these points, which repeated these, with greater brevity, for the editor. To keep things clear and concise in this response we have treated these both together and have directed our replies to his detailed review in the pdf, as this covers all of the points he raises.

**Tim Cullen – Comments on PDF**

1. Reconstruction of the eroded parts of the sedimentary system. You point out in the supplementary material, and it is evident from seismic section in Figure 2b that large portion of the central region of the study area stratigraphy between 5.5 Ma – 3.5 Ma has been eroded. Yet Figure 2c, and the maps in the supplementary information refer to channel crossings in this time interval – how were the position of them and the strain-rate for those fault segments at that time constructed/constrained given the erosion off the hangingwalls of faults 13, 15 and 17? This is a good point. A new Figure S2 has been included in the supplementary material which shows that the erosion in the central part of the fold belt did not impact our ability to image the channels up dip and down dip of it, however channels were indeed not interpreted where the stratigraphy had been eroded. This is why we used a formal statistical approach. We have inferred only one crossing to occur within the eroded area (indicated in Fig. S2), which is well evidenced by the preserved channels on either side and which does not impact the statistical results even if it were discounted. Fault strains were reconstructed as described in Jolly et al., 2016; by projecting the horizons across the scarp and over the structure, reconstructing the shape of the structure. We have added some text in the supplementary information but the reader is properly referred to Jolly et al., 2016 and Pizzi et al., 2020 for the published approach.

2. Strain rates for faults which do not break the surface at a given time: Perhaps in the supplementary information, but preferably within the portion of the text that refers to calculating strain rates, it would be good to add a line of how the blind faults are handled in this analysis. Is the shortening at the folds above them (e.g. for the 5.5 Ma horizon above F.21) calculated to produce a strain and placed accordingly or are they treated as 0 strain? If so, was there a control/test to show that this was negligible enough to be assumed as zero strain and could this be included in the supplementary information? The strain rate analysis method is fully published in Jolly et al., 2016 and Pizzi et al., 2020. We have clarified in Section 2 of the supplementary material that “*Strain and strain rates were calculated using a modified version of the line-length balancing technique following the methodology described in Jolly et al. (2016) and improved further by Pizzi et al. (2020). This methodology included the measure of shortening and strain of both the faulted and folded horizons to allow deformation to be consistently quantified beyond and above the tip of blind thrusts. Strain and shortening rates for the thrust-folds found within the central area were reconstructed by projecting the horizons across the scarp and over the structure while maintaining the overall shape of the structure (Jolly et al., 2016)*” We calculated strains for both the faulted and folded horizons beyond the tip of blind thrusts, therefore no control test was needed. Zero-strain means that no folding is measured.

3. Further explanation that justifies the use of the “total lengths” of faults in generating histograms. There is a portion of the description of that method for generating the histograms that comes across as a little confusing/comes out of the blue regarding the need to include the maximum length of all the faults in the array (Line 95-96). Would you be able to explain why this is an important part of the analysis to consider all the faults and sum them and have a maximum at any given time? (is this just a routine part of the statistical analysis? It seems counterintuitive – e.g. why would a channel crossing a given fault in one place, care about

the length of a fault segment it goes nowhere near, very far updip/down dip?). I certainly don't disagree with the methodology, which produces an excellent quantitative description of the evolution you describe. We have clarified the purpose in the main text (L87) to state that "*Histograms were derived of (i) the strain rate recorded at channel crossings and (ii) the strain rate as a function of the total length of active fault segments, to capture the strain rate distribution for the overall fault array relative to the channel-fault intersections*". Further to the reviewer's question - our method is a required part of the statistical analysis. The reason is that we need to have a statistical distribution of the strain rate in the fault array as a whole. We have numerous fault segments of differing lengths, with differing strain rates for each interval. To get the distribution of strain rate in any one interval, one is required to multiply the strain rate in each segment by its length - and then sum these. To get the cumulative distribution over the study period we add all the intervals together. We then ask whether the typical strain rate in the fault array is different from the distribution of strain rates at the fault-channel crossings. We don't just work out the strain rate at the fault channel intersections because the point is that we need to evaluate if that is different (or not!) from what the faults are doing as a whole. The K-S test is a standard, formal way of evaluating whether the two distributions are similar and we show they are unambiguously are not. We think the main text is now explicit on this point, but we have also added a more text to section 4 of the supplementary material too to explain this further for interested readers who wish to know more background. The K-S test is a standard statistical method, so we feel it is not appropriate to introduce this from first principles within the Geology manuscript itself.

4. Clarification of Figure 2c I would suggest changing the colour of the black rings on Figure 2c to avoid confusion with the colour scale for  $>7\%/Ma$ . This initially was quite confusing...A minor point, but one that may need addressing given this is the principal 'data' figure, and to avoid any disgruntled readers! **Good point – we have edited Fig. 2c to address this comment.**

5. Frequency and importance of reference to unpublished material Understandably much of this work uses pre-existing interpretations from a structural model in Pizzi et al. (2020), and observations and interpretations in Pizzi (2019). I'm a little concerned that readers, and myself, do not have the opportunity to chase these as the necessary data, observations and interpretations referred to from Pizzi (2019) is not open or available to see. I tried searching to see if this were in some form of online repository, EarthArxiv or similar but could not find them after a reasonable amount of time. (If this is out there somewhere and you refer to it I would suggest flagging up to the reader where this can be found). My suggestion here would be to include a map figuresimilar that of S4 (which I assume is in the thesis?) but focussing on the seismic data that governed the positions of the channels, and refer to that instead of Pizzi (2019). Similarly, the restoration which provides the strain rates, would benefit from further detail in the supplementary information to address Point 3 above with regards to blind faults. Additionally, please include the constraints for the age model of the horizons, given their importance in determining strain rate in the Supplementary information. **This is a good point and we take it seriously.** The PhD thesis of Pizzi is a fully-reviewed, corrected and approved thesis that was submitted to Imperial College Library in 2019. **We have liaised with library services to make sure it is fully available online, open access from Imperial College London, and it has its own doi: doi.org/10.25560/85679.** It is available to download on the official Imperial library website: <https://spiral.imperial.ac.uk/handle/10044/1/85679> . Rather than replicating wholesale the thesis in the supplementary material, we have judiciously added a couple of new ancillary figures to illustrate the channel imaging (see comments above). If readers are particularly interested in the imaging (which is not the primary focus of this paper), they are encouraged to assess the seismic amplitude maps directly on chapter 5 of Pizzi 2019 as it is not practical to make a figure similar to old Fig S4 (new S6) for the amplitudes as they would not be large enough to be understood. The full methodology used for the strain-analysis, as well as the age constraints is published Jolly et al., 2016 and Pizzi et al., 2020 so it is unnecessary to repeat all of this material in the supplementary information. However the point regarding how strain was calculated above blind thrusts has been addressed in section 2 and included as well as the source of the age constraints.



# New statistical quantification of the impact of active deformation on the distribution of submarine channels

Marco Pizzi<sup>1,2</sup>, Alexander C. Whittaker<sup>1\*</sup>, Lidia Lonergan<sup>1</sup>, Mike Mayall<sup>1</sup>, W. Hamish Mitchell<sup>1</sup>.

<sup>1</sup>Department of Earth Science & Engineering, Imperial College, London SW7 2AZ, UK.  
<sup>\*</sup>Corresponding author.

<sup>2</sup>now at: Fugro GB Marine Limited, Victory House, Trafalgar Wharf (Unit 16), Hamilton Road, Portsmouth, PO6 4PX, UK.

## ABSTRACT

Submarine channel systems play a crucial role in governing the delivery of sediments and pollutants such as plastics from the shelf edge to deep-water. Understanding their distribution in space and time is important to constrain the locus, magnitude and characteristics of deep-water sedimentation, and to predict stratigraphic architectures and depositional facies. ~~Here,~~ Using 3D seismic reflection data covering the outer fold and thrust belt of the Niger Delta, we determined the ~~distributions and~~ pathways of Miocene to Pliocene channels that crossed eleven fold-thrust structures, at 173 locations, for which the temporal and spatial evolution of strain rates have been constrained over 11 Myr. We use a statistical approach to quantify strain and shortening rate ~~distributions~~ recorded where channels have crossed structures, compared to the fault array as a whole, ~~during the growth history of the fold and thrust belt.~~ Our results prove unambiguously that these distributions are different. in response to increasing deformation rates submarine channels are driven to locations of lower strain rates. The median strain rate where channels cross faults is < 0.6%/My (~40m/My), 2.5 times lower than the median strain rate of active fault segments (1.5%/My) with a marked reduction in the number of channel-fault crossings where fault strain rates exceed 1% Ma. Our results quantify the sensitivity of submarine channels to active deformation at a population level for the first time, and enable us with a marked reduction in the number of channel-fault crossings. Consequently, strain analyses are an important tool to predict the temporal and spatial routing ~~and distribution~~ of submarine channels affected by structurally-driven topography.

**Style Definition:** Heading 3: Indent: Hanging: 1.5", Outline numbered + Level: 3 + Numbering Style: 1, 2, 3, ... + Start at: 1 + Alignment: Left + Aligned at: 1" + Tab after: 1.5" + Indent at: 1.5", Tab stops: 0.39", List tab + Not at 1.5"

**Formatted:** Numbering: Continuous

34

## 35 INTRODUCTION

36 Submarine channel systems form the largest sedimentary deposits on Earth (Talling et al.,  
37 2015) and control the delivery of sediment, organic material and ~~micro-and-macro~~plastics  
38 from the continents to deep water (Babonneau et al., 2002; Covault et al., 2016; Sweet and  
39 Blum, 2016; Kane & Clare, 2019). Understanding their distribution in space and time is  
40 important to constrain the locus, magnitude and completeness of deep-water stratigraphy, and  
41 to predict stratigraphic architectures and reservoir facies (Mayall et al., 2006, 2010; Sømme  
42 et al. 2009; Covault et al., 2016). Submarine channels are often found on passive margins that  
43 deform due to gravity tectonics, causing the growth of folds and thrusts at the toe-of-slope  
44 (Damuth 1994; Corredor et al 2005; Jolly et al., 2016; Don et al., 2019). The growth of these  
45 structures is expressed by the creation of seabed topography that modifies the slope gradient  
46 and creates tortuous corridors, which can be exploited by ~~the submarine~~ channels (Smith,  
47 2004; Callec et al., 2010; Bourget et al., 2011; Howlett et al., 2019) (Fig 1). ~~Although it~~ is  
48 often ~~suggested~~assumed that submarine channels ~~, particularly those active coeval with~~  
49 ~~deformation,~~ are sensitive to topographic changes driven by active deformation shortening  
50 (Pirmez et al., 2000; Ferry et al., 2005), individual case studies to-date show a wide range of  
51 channel responses to growing structure (Clark and Cartwright, 2009, 2012; Jolly et al., 2016;  
52 Mitchell et al., 2020). While theory and empirical observation suggest relationships between  
53 increased slope, structural uplift and channel incision/deflection, the sensitivity of  
54 submarine channels to the magnitude and rate of active deformation has never been  
55 comprehensively quantified. Several studies have indicated a close link between increased  
56 slope, structural uplift and greater channel incision/deflection (Clark and Cartwright, 2009,  
57 Mayall et al., 2010; Deptuck et al., 2012; Jolly et al., 2017; Mitchell et al., 2020). In  
58 particular, analysis of stratal relationships and isopach maps indicates that locations where  
59 channels cross growing structures may be dependent upon along-strike structural variations  
60 and the relative rates of uplift and sediment accumulation (Clark and Cartwright 2012, Jolly  
61 et al., 2016). No study has attempted a robust statistical analysis of a large number of  
62 submarine channel-structure crossings in time and space, where the deformation rates are  
63 measured independently. Here we address this challenge.~~Here we address this~~  
64 ~~challenge.~~However, this issue has typically been addressed on a qualitative or case-study  
65 basis, where examples of individual channels are shown to be diverted around structures,  
66 whose deformation rate may (or may not) have been quantified (Clark and Cartwright, 2009,

67 ~~2012; Mitchell et al., 2020). No study has attempted a statistical analysis of a large number of~~  
68 ~~submarine channel structure crossings in time and space, where the deformation rates are~~  
69 ~~measured independently. Here we address this challenge.~~

70  
71 We use 3D seismic reflection data on the southern lobe of the Niger Delta (Fig. 1), to  
72 determine the frequency distribution of Miocene to Pliocene channel systems where they  
73 cross gravity-driven fold-thrusts ~~\_for which the temporal and spatial evolution of strain~~  
74 ~~are whose strain rate evolution is exceptionally~~ well constrained (Pizzi, 2019; Pizzi et al.,  
75 2020). We quantify the strain rates where channels cross structures, ~~and compare compared~~  
76 to the fault array as a whole, throughout the ~~11 Myr~~-growth history of the fold and thrust belt.  
77 ~~For the first time, we~~ Our data set therefore allows us to test statistically the hypothesis that  
78 submarine channels are sensitive to on-going deformation near the seabed, ~~and quantify~~  
79 ~~when, where and with what probability submarine channels can cross active structures. :-~~

80

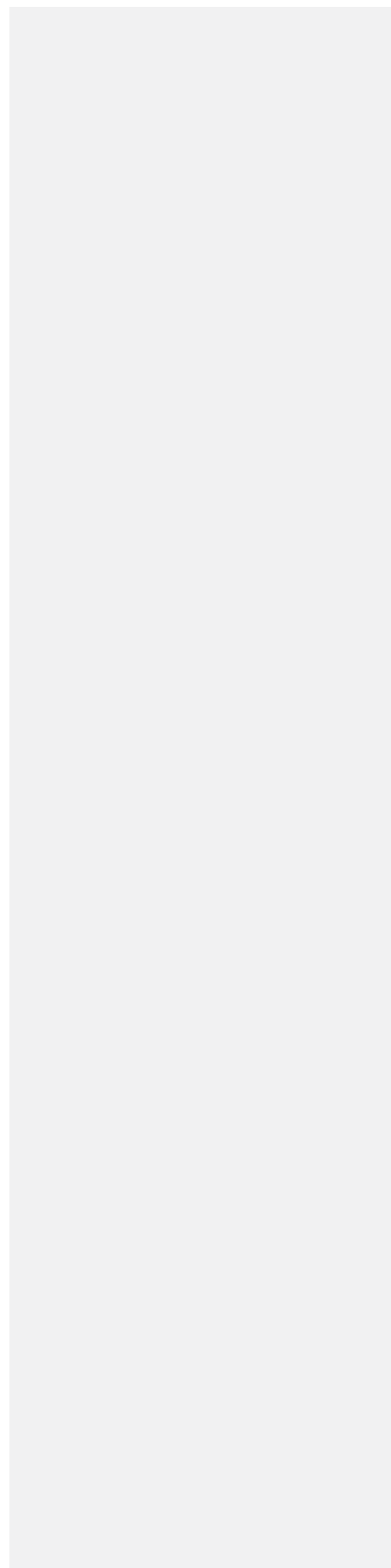
## 81 **STUDY AREA AND METHODS**

82 The Niger Delta (Fig. 1A) has ~~a total an~~ area of 140,000 km<sup>2</sup> with 12 km of sediments  
83 deposited since the Early Eocene (Damuth, 1994). The rapid advance of the delta ~~front~~ above  
84 slope and pro-delta shale units facilitated the gravitational collapse of the system since the  
85 Miocene (e.g. Morgan, 2003; Bilotti and Shaw, 2005). The gravity failure was  
86 accommodated by extensional tectonics on up-dip areas ~~of the delta~~, and shortening towards  
87 the delta toe (Damuth, 1994; Fig. 1).

88

89 The study area is located on the lower slope of the delta (Fig. 1A) where numerous submarine  
90 channel systems have interacted with contractional structures from the Miocene to the present  
91 day (Fig. 1B) (Jolly et al., 2016, 2017; Mitchell et al., 2020). Using 3D seismic data ~~from~~  
92 ~~PGS~~, Pizzi (2019) and Pizzi et al. (2020) comprehensively quantified the structural evolution  
93 of eleven thrusts on the southern lobe of the Niger Delta (thrusts 12 to 22, Fig. 2A, B). ~~-The~~  
94 thrusts initiated at or before 15 Ma, with strain varying ~~both~~ between structures and along  
95 strike, and also through time. Increases in fault length, associated with along-strike  
96 interaction and linkage, mostly occurred prior to 7.4 Ma. Deformation increased significantly  
97 between 9.5-6.5 Ma with ~~typical~~ shortening rates ~~of > 200 -400~~-m/Mya. We exploit the  
98 unique availability of detailed maps of strain rate evolution (Pizzi, 2019; Pizzi et al., 2020;  
99 *supplementary material*), such as the 5.5-3.7 Ma interval shown in Fig. 2C, as a well-

100 constrained template of deformation rate and magnitude to test the sensitivity of submarine  
101 channels to active deformation.  
102



103 Deep-water slope channels crossing coeval active fault segments were identified within six  
104 temporal intervals from 15 to 3.7 Ma (Pizzi et al., 2020; Table S1) using standard seismic  
105 stratigraphic techniques including multiple seismic sections and RMS amplitude extractions  
106 (*supplementary material*, Figs. S2-S5, S3, Pizzi, 2019). For each interval, channel courses  
107 were overlain on the corresponding strain rate map, to record the fault strain rate at each  
108 channel-fault intersection, as shown in Figure 2C. This yielded 173 channel crossings  
109 between 15 and 3.7 Ma, noting that a single channel may cross multiple structures (Fig. S64).  
110 ~~Histograms-Histograms~~ were derived of (i) the strain rate recorded at ~~each~~ channel crossings  
111 ~~and (ii) -for each of the six time intervals. Analogous distributions of the strain rate as a~~  
112 ~~function of the~~ total length of active fault segments, ~~deforming at a given strain rate, were~~  
113 ~~compiled for each time interval and for the entire period of study to capture the strain rate~~  
114 ~~distribution for the overall fault array relative to the channel-fault intersections (Fig. 3A, B).~~  
115 The maximum length of all the faults in the array for any one time interval was 417 km. The  
116 mean strain rate for channel-fault intersections and the fault array at each time interval were  
117 recorded. The results for each unit were summed and normalized to derive three cumulative  
118 density functions as a function of strain rate; one of the number of channel crossings, and two  
119 depicting the cumulative distribution of fault segment lengths, with and without segments of  
120 zero strain, which were subsequently or previously active (Fig 3C). ~~We compared these~~  
121 ~~distributions to test the hypothesis that submarine channels preferentially exploited crossing~~  
122 ~~points located at low strain rate in the evolving fault array. To confirm that test the hypothesis~~  
123 ~~that~~ the strain rates ~~for at~~ submarine channel-fault crossings are significantly different from  
124 ~~fault~~ strain rates in the fault array, it must be demonstrated they ~~could not be~~ drawn  
125 from the same underlying distribution, given we have not sampled all possible channels  
126 crossing faults ~~o~~in the southern lobe of the Niger Delta. We used a two sample Kolmogorov-  
127 Smirnov test (K-S test) to evaluate this. The null hypothesis - that the ~~cumulative~~ distribution  
128 of strain rates at channel crossing ~~points~~ s is the same as the distribution of fault segment  
129 strain rates - was tested at the 95% confidence interval (*supplementary material*, Tables S2,  
130 S3). ~~We perform the K-S test for channel crossings at the scale of the whole fault array~~  
131 ~~rather than on individual or groups of structures across strike to avoid arbitrary grouping of~~  
132 ~~data that may pre-determine the results and to obtain a statistically valid sample size.~~

133

## 134 RESULTS

135 ~~By summing the fault lengths for the 6 intervals we~~We obtained a cumulative total of 2505  
136 km of faults active in the period between 15 Ma to 3.7 Ma (Fig. 3A; Table S3). All segments  
137 were active between 7.4 and 6.5 Ma; in the earlier and later intervals some were inactive  
138 (Pizzi et al., 2020, Fig. S64). ~~The Modal strain rates of majority of thrust segments (847 km)~~  
139 ~~had strain rates in the range of 0 to 1 %/MaMy (~70 m/My) are documented for the thrusts,~~  
140 with ~~progressively fewer a significant proportion~~ at higher strain rates (Fig. 3A). A more  
141 conservative approach, excluding zero-strain rate segments for any time interval, yields 2139  
142 km of active fault segments ~~in the period between 15 Ma and 3.7 Ma over the period.~~  
143 Presented as cumulative density functions (Fig. 3C), 50% of the fault segments were active at  
144 ~~strain~~ rates of more than 1.5 %/MaMy in the period between 15 Ma and 3.7 Ma (red curve)  
145 or at more than 1.1 %/MaMy if zero strain rate segments are included (dashed red curve).

146  
147 ~~The results for the~~The channel-crossing fault intersections as a function of strain rate (Fig.  
148 3B) show a markedly different distribution. The modal number of channels crossings  
149 occurred for strain rates up to 1%/MaMy; ~~and~~ an additional 48 crossings occurred over fault  
150 segments that were then inactive. However fewer crossings are recorded at higher strain rates.  
151 Only 4 channels cross structures with ~~strain~~-rates  $> 5\%/MaMy$ , and none are documented for  
152 strain rates  $> 7\%/MaMy$ . Significantly, the cumulative density function (Fig. 3C) shows that  
153 50% of the crossings occurred for strain rates smaller than  $0.6\%/MaMy$ , a value 2.5 times  
154 ~~markedly~~ less than the median of the active fault segments ( $1.5\%/MaMy$ ). Consequently, the  
155 distribution of channels is skewed towards smaller values of strain rate. A K-S test at the 95%  
156 confidence interval confirms ~~that~~ we can reject the null hypothesis that the two observed  
157 distributions sample the same underlying distribution ~~(Table S3)~~. Indeed, our results show  
158 that we can reject the null hypothesis at ~~the a higher~~ 99.9% confidence interval ~~(Table S3)~~. ~~In~~  
159 ~~other words~~Consequently, our data demonstrate unambiguously that submarine channels on a  
160 structured slope statistically exploit ~~locations of~~ lower strain rate to cross evolving faults  
161 over ~~a time period of 11 MaMy period, and enables us to quantify for the first time how this~~  
162 ~~distribution differs from strain rates in a fault array as a whole.-~~

### 164 1. — TEMPORAL EVOLUTION OF STRAIN RATES AND CHANNEL CROSSINGS

165 ~~The evolution of mean Mean fault~~ strain rate ~~in the fault array for in~~ each time interval  
166 ~~produces a pattern of increasing deformation rate~~increases until ca. 7 Ma, followed by

167 decreasing strain rate thereafter (Fig. 4A). The faults deformed at an average rate of 0.5  
168 %/~~Ma-My~~ from 15 to 9.5 Ma, reached a peak of 3.3 %/~~Ma-My~~ (~230 m/~~MaMy~~) in the 7.4 to  
169 6.5 Ma interval, and decreased to ca. 1.5 %/~~Ma-My~~ by 4 Ma. Mean strain rates recorded at  
170 the channel crossings (~~Fig. 4A~~) follow a similar pattern. However, while initially values were  
171 close to those for the whole fault array, they subsequently diverged when strain rates  
172 exceeded ~1%/My threshold, with channel crossings occurring at lower values of strain rate  
173 than the fault array mean. The number of channel crossings progressively decreased from 15  
174 Ma to the 7.4-6.5 Ma interval and then increased thereafter (Fig. 4B). However, the trend is  
175 asymmetric such that a slow decrease in the number of channel crossings is followed by a  
176 marked increase when deformation slows after 6.5 Ma. Despite the reduction in shortening  
177 rate, the mean strain rate at channel crossings remains suppressed relative to that of the fault  
178 array for the youngest units 2 and 1 (Fig. 4A) indicating-showing a fast response of channel  
179 systems to changing boundary conditions, with new channels entering the area rapidly  
180 locating themselves so as to cross fault segments with lower strain rates.

181

## 182 DISCUSSION

183 ~~Our results demonstrate that two~~Two-thirds of all channel-fault intersections ~~with active~~  
184 ~~structures~~ over a period of ca. 11 Myr ~~have~~ occurred at strain rates lower than 1%/~~Ma-My~~,  
185 while the median strain rate of the array over the period was 1.5%/~~Ma-My~~ – a statistically  
186 significant difference (Fig. 3). ~~The distributions of channel crossings and active faults as a~~  
187 ~~function of strain rate are statistically different.~~While individual examples of channels  
188 crossing fast deforming faults can be found, our results are powerful because they quantify  
189 how the probability of channels crossing high strain rate structures reduces progressively as  
190 fault strain rates grow beyond 1%/My. We therefore caution against generalising models of  
191 channel behaviour from individual examples. ~~As the~~The evolution of strain rates at the  
192 channel crossings mirrors, but is persistently lower than that of the fault array (Fig. 4A). ~~we~~  
193 ~~argue that~~Consequently, ~~although while~~ submarine channel crossings are forced to follow the  
194 tectonic history of the area, the channels during each time interval actively locate to, or ~~are~~  
195 ~~remained~~ pinned at, ~~at~~ points of lower strain rate to cross growing structures. ~~In this study,~~  
196 ~~strain rates of 1.5%/Ma translate into shortening of 100 m/Ma.~~We hypothesise that the  
197 control is structurally-mediated paleo-topography, the growth of which is ~~likely~~ enhanced by  
198 thrust fault linkage (see Pizzi et al., 2020). Although converting shortening rates into uplift  
199 rates requires assumptions (c.f Hardy and Poblet, 2005; Jolly et al., 2016; Mitchell et al.,

Formatted: Font: 12 pt

Formatted: Font: 12 pt

Formatted: Font: 12 pt

Formatted: Font: 12 pt

Formatted: Font: 12 pt, Italic

Formatted: Font: 12 pt

Formatted: Font: 12 pt

200 2020), these shortening rates imply crestal uplift rates of equivalent magnitude for ~~single step~~  
201 flexural-slip fault propagation folds, and have ~~previously~~ been shown to be sufficient to  
202 deflect sub-modern seabed channels on the Niger Delta (Jolly et al., 2017).

203  
204 That the number of channel crossings decreases for greater values of strain rate and increases  
205 as soon as strain rates decrease (Fig.4B) reflects the reduced number of ~~possible~~ pathways  
206 that channels can realistically exploit to reach more distal areas during times of intense  
207 structural deformation and the potential for sediment ponding up-dip of structures (Clark and  
208 Cartwright, 2012; Pizzi, 2019) (Fig. 2c; Fig. S4). Therefore, not only are channels deflected  
209 by deforming structures, even for relatively low strain rates, but the network is focused at a

210 small number of crossing points when deformation rates are high, ~~tracking the deformation~~  
211 ~~history of the area~~ (Fig 2c). ~~However, when mean strain rates fall, new channels rapidly~~  
212 ~~locate themselves at additional fault crossing points that still have lower-than-average~~  
213 ~~deformation rates~~ However, when mean strain rates fall, new channels locate themselves  
214 rapidly at additional fault crossing points that still have lower-than-average deformation rates.

215 ~~We argue that in this scenario more crossing points become available to be exploited,~~  
216 ~~enhancing the probability that new channels find crossings with lower strain/shortening rates~~  
217 ~~—Consequently, the locus and magnitude of sediment supply to deep water basins is~~

218 predictably influenced by the 4D growth history of contractional faults on structured margins  
219 and the incompleteness of marine sedimentary records down-system of interacting faults ~~is~~  
220 ~~expected to will~~ track the strain rate evolution of the array. The statistical distributions and

221 methodology presented here could be used to predict submarine channel routing on structured  
222 slopes, even where seismic imaging is limited. Consequently, Our results therefore  
223 ~~demonstrate that this~~ ~~this~~ type of ~~structural template analysis~~ ~~—~~ serves as a powerful tool to  
224 ~~understand reconstruct both~~ sediment confinement and the routing of sands and pollutants to  
225 deep water.

## 226 227 **CONCLUSIONS**

228 From a statistical analysis of 173 submarine channel-fault crossings in the deep-water Niger  
229 Delta, and a cumulative 2505 km of fault segments for which strain rates have been  
230 calculated over an 11 Myr history, ~~this analysis we~~ shows that:

231 1. Distributions of fault array strain rate and submarine channel-fault crossing strain rate are  
232 statistically different using a two-sample K-S test. The median strain rate where channels

Formatted: Font: 12 pt

Formatted: Font: 12 pt

Formatted: Font: 12 pt



233 cross faults is  $< 0.6\%/Ma$ , ~~significantly lower than the 2.5 times lower than the~~ median strain  
234 ~~value deformation rate~~ of active fault segments ( $1.5\%/My$ ;  $\sim 100m/My$ );

235  
236 ~~2. Our results prove statistically that at a population level, channels exploit available~~  
237 ~~locations of lower strain rate to cross active structures, although the mean strain rate at~~  
238 ~~crossing points tracks the deformation history of the area; we hypothesise this control is~~  
239 ~~exerted by fault-induced topography on the sea-bed. The cumulative density functions of~~  
240 ~~fault array strain rate and channel crossing point strain rate are statistically different at the~~  
241 ~~95% confidence interval using a two sample K-S test.~~

242 ~~3. Submarine channels are statistically shown to exploit available zones of lower strain rate~~  
243 ~~along the strike of faults; The submarine channel network focusses into fewer channels~~  
244 ~~crossing faults at higher deformation strain rates rates. However as soon as the deformation~~  
245 ~~rates decrease, submarine channels rapidly spread across the region, with new channels~~  
246 ~~crossing faults in areas locate themselves in areas of relatively lower strain rate. although the~~  
247 ~~mean strain rate recorded at fault crossing points tracks the deformation history of the area;~~  
248 ~~we hypothesise this control is exerted by fault induced topography on the sea bed.~~

249 ~~4. Our results caution against the use of individual channel examples to deduce submarine~~  
250 ~~channel sensitivity to active deformation; illustrate how population statistics give rise to a~~  
251 ~~step-change in our understanding of typical submarine channel behaviour; and demonstrate~~  
252 ~~that strain rate analyses are a powerful tool for predicting the routing of sands and pollutants~~  
253 ~~to deep water. The submarine channel network focusses into fewer channels crossing faults at~~  
254 ~~higher deformation rates. However as soon as the deformation rates decrease, submarine~~  
255 ~~channels rapidly spread across the region, with new channels crossing faults in areas of~~  
256 ~~relatively low strain rate.~~

257  
258 **ACKNOWLEDGEMENTS**

259 MP was funded by the NERC CDT in Oil & Gas. Data ~~for the project~~ was provided by PGS  
260 and the Nigerian Petroleum Directorate. We thank ~~E. Taylor and R. Lamb and E. Taylor~~ for  
261 ~~facilitating access to data access. We and~~ acknowledge software donations from Landmark-  
262 Halliburton and StructureSolver™. ~~We thank Tim Cullen and two anonymous reviewers for~~  
263 ~~their constructive comments.~~

264

265 **FIGURE CAPTIONS**

266 | Figure 1: – A) Location and ~~structural~~ setting of the Niger Delta. Study area shown as orange  
267 | box. B) Three-dimensional image from the south of the study area showing submarine  
268 | channels (dashed white lines) interacting with folds (black dashed lines) of the outer fold-  
269 | and-thrust belt. Study interval of ~15-3.7 Ma highlighted in yellow.

270  
271 | Figure 2 A) Depth-structure map of the 9.5 Ma horizon showing eleven thrusts, labelled 12-  
272 | 22, deforming the lower slope. (B) Cross-section through the seismic data showing ~~the~~ folds  
273 | and mapped horizons, adapted from Pizzi et al., (2020). ~~See-Fig. S2 shows the uninterpreted~~  
274 | seismic section. C) Example ~~of a~~ strain rate map for the 5.5-3.7 Ma interval, showing spatial  
275 | variation in fault segment strain rate. Strain was calculated using a normalised line length of 7  
276 | km. Submarine channel systems were mapped and their crossing locations and associated  
277 | strain rate (circles) were recorded (see Supplementary material).

278  
279 | Figure 3: Histograms of:- (A) Total kilometres of active fault segments ~~for a given range of~~  
280 | ~~and (strain rate over 11 Myr. Most of the faults were active in 0-1 %/Ma range.~~ (B) Total  
281 | number of channel-fault crossings against for a given range of strain rate over 11 Myr fault  
282 | array history. - (C) Cumulative density functions ~~derived~~ from the histograms above for the  
283 | strain rate of ~~all~~ active faults segments (red line), those including segments of zero strain (red  
284 | dashed line); and strain rate of channel-fault crossings. 50% of channels exploited strain rates  
285 | <0.6%/Ma, while 50% of faults deformed at rates above 1.5%/Ma. ~~The distributions of~~  
286 | ~~channels and faults are statistically different, indicating that channels seek the locations of~~  
287 | ~~lower strain rate to cross active structures.~~

288  
289 | Figure 4: ~~For the six studied time intervals:-~~ (A) Mean shortening and strain rates against time  
290 | for the fault array as a whole (~~red line~~) and for channel-fault ~~intersections~~ crossings. (B)  
291 | Number of channel crossings and strain rate for the fault array as a whole against time.  
292 | Number of channel crossings at 5.5 Ma is a minimum estimate as some poorly imaged  
293 | channels are not included.

294  
295

296 **REFERENCES CITED**

- 297 Babonneau, N., Savoye, B., Cremer, M., and Klein, B. 2002, Morphology and architecture of  
298 the present canyon and channel system of the Zaire deep-sea fan. *Marine and Petroleum*  
299 *Geology*, v. 19(4), p. 445-467.
- 300 Bourget, J., Zaragosi, S., Ellouz-zimmermann, N., Mouchot, N., Garlan, T., Schneider, J. L.,  
301 and Lallemand, S. 2011, Turbidite system architecture and sedimentary processes along  
302 topographically complex slopes: the Makran convergent margin. *Sedimentology*, v.  
303 58(2), p. 376-406.
- 304 Bilotti, F. and Shaw, J.H., 2005, Deep-water Niger Delta fold and thrust belt modeled as a  
305 critical-taper wedge: The influence of elevated basal fluid pressure on structural styles.  
306 *AAPG Bulletin*, v. 89(11), p.1475-1491.
- 307 Callec, Y., Deville, E., Desaubliaux, G., Griboulard, R., Huyghe, P., Mascle, A., and  
308 Schmitz, J. 2010, The Orinoco turbidite system: Tectonic controls on sea-floor  
309 morphology and sedimentation. *AAPG bulletin*, v. 94(6), p. 869-887.
- 310 Corredor, F., Shaw, J.H. and Bilotti, F., 2005, Structural styles in the deep-water fold and  
311 thrust belts of the Niger Delta. *AAPG Bulletin*, v. 89(6), p. 753-780.
- 312 Covault, J. A., Sylvester, Z., Hubbard, S. M., Jobe, Z. R., and Sech, R. P., 2016, The  
313 stratigraphic record of submarine-channel evolution: *The Sedimentary Record*, v. 14, p.  
314 4-11.
- 315 Clark, I. R., and Cartwright, J. A. 2009, Interactions between submarine channel systems and  
316 deformation in deepwater fold belts: Examples from the Levant Basin, Eastern  
317 Mediterranean sea. *Marine and Petroleum Geology*, v. 26(8), p. 1465-1482.
- 318 Clark, I. and J. Cartwright, 2012, Interactions between coeval sedimentation and deformation  
319 from the Niger Delta deepwater fold belt, *SEPM Special Publication 99*, p.243-267.
- 320 Damuth, J., 1994, Neogene gravity tectonics and depositional processes on the deep Niger  
321 Delta continental margin, *Marine and Petroleum Geology*, v. 11, p.320-346.
- 322 Deptuck, M. E., Sylvester, Z., and O'Byrne, C. 2012, Pleistocene seascape evolution above a  
323 "simple" stepped slope, western Niger Delta. Application of the principles of seismic  
324 geomorphology to continental slope and base-of-slope systems: Case studies from sea  
325 floor and near-sea floor analog: *SEPM Special Publication 99*, p. 199-222.
- 326 Don, J., Shaw, J. H., Plesch, A., Bridgwater, D. D., and Lufadeju, G. 2019, Characterizing the  
327 growth of structures in three dimensions using patterns of deep-water fan and channel  
328 systems. *AAPG Bulletin*, v. 104 (1), p. 177-203.

329 Ferry, J. N., Mulder, T., Parize, O., & Raillard, S. 2005, Concept of equilibrium profile in  
330 deep-water turbidite system: effects of local physiographic changes on the nature of  
331 sedimentary process and the geometries of deposits. Geological Society of London  
332 Special Publication, 244(1), p. 181-193.

333 Hardy, S., and Poblet, J. 2005, A method for relating fault geometry, slip rate and uplift data  
334 above fault-propagation folds. Basin Research, v. 17(3), p. 417-424.

335 Howlett, D. M., Ge, Z., Nemeč, W., Gawthorpe, R. L., Rotevatn, A., and Jackson, C. A. L.  
336 2019, Response of unconfined turbidity current to deep-water fold and thrust belt  
337 topography: Orthogonal incidence on solitary and segmented folds. Sedimentology, v.  
338 66(6), p. 2425-2454.

339 Jolly, B.A., Lonergan, L. and Whittaker, A.C., 2016, Growth history of fault-related folds and  
340 interaction with seabed channels in the toe-thrust region of the deep-water Niger delta.  
341 Marine and Petroleum Geology, v. 70, p. 58-76.

342 Jolly, B.A., Whittaker, A.C. and Lonergan, L., 2017, Quantifying the geomorphic response of  
343 modern submarine channels to actively growing folds and thrusts, deep-water Niger  
344 Delta. Geological Society of America Bulletin, v. 129, p. 1123-1139.

345 Kane, I. A., and Clare, M.A., 2019, Dispersion, Accumulation, and the Ultimate Fate of  
346 Microplastics in Deep-Marine Environments: A Review and Future Directions, Frontiers  
347 in Earth Sciences, v. 7, A80, doi.org/10.3389/feart.2019.00080.

348 Mayall, M., Jones, E., and Casey, M. 2006, Turbidite channel reservoirs—Key elements in  
349 facies prediction and effective development. Marine and Petroleum Geology, v. 23(8), p.  
350 821-841.

351 Mayall, M., Lonergan, L., Bowman, A., James, S., Mills, K., Primmer, T., and Skeene, R.  
352 2010, The response of turbidite slope channels to growth-induced seabed topography.  
353 AAPG bulletin, v. 94(7), p. 1011-1030.

354 Mitchell, W. H., Whittaker, A., Mayall, M., Lonergan, L., and Pizzi, M., 2020, Quantifying  
355 the relationship between structural deformation and the morphology of submarine  
356 channels on the Niger Delta continental slope, Basin Research,  
357 doi.org/10.1111/bre.12460 (in press).

358 Morgan, R., 2003, Prospectivity in ultradeep water: the case for petroleum generation and  
359 migration within the outer parts of the Niger Delta apron. Geological Society of London,  
360 Special Publication, 207, p.151-164.

361 Pirmez, C., Beaubouef, R. T., Friedmann, S. J., Mohrig, D. C., and Weimer, P. 2000,  
362 Equilibrium profile and baselevel in submarine channels: examples from Late

363 Pleistocene systems and implications for the architecture of deepwater reservoirs. In  
364 Global deep-water reservoirs: Gulf Coast Section SEPM Foundation 20th Annual Bob F.  
365 Perkins Research Conference, p. 782-805. ISBN: 9781605603322.

366 Pizzi, M. 2019. Quantification of tectonic controls on the distribution and architecture of  
367 deep-water facies during the growth of the toe-thrusts region of the Niger Delta, PhD  
368 thesis, Imperial College London, 238 pp. doi.org/10.25560/85679.

369 Pizzi, M., Lonergan, L., Whittaker, A.C., and Mayall, M., 2020, Growth of a thrust fault  
370 array in space and time: An example from the deep-water Niger delta: *Journal of*  
371 *Structural Geology*, v. 137, 104088, 10.1016/j.jsg.2020.104088.

372 Sømme, T. O., Helland-Hansen, W., Martinsen, O. J., and Thurmond, J. B. 2009,  
373 Relationships between morphological and sedimentological parameters in source-to-sink  
374 systems: a basis for predicting semi-quantitative characteristics in subsurface systems.  
375 *Basin Research*, v. 21(4), p. 361-387.

376 Smith, R. U. 2004, Silled sub-basins to connected tortuous corridors: Sediment distribution  
377 systems on topographically complex sub-aqueous slopes. Geological Society of London,  
378 Special Publication 222, p. 23-43.

379 Sweet, M. L., and Blum, M. D., 2016, Connections between fluvial to shallow marine  
380 environments and submarine canyons: Implications for sediment transfer to deep water.  
381 *Journal of Sedimentary Research*, v. 86(10), p. 1147-1162.

382 Talling, P., J. Allin, D.A. Armitage, R.W.C. Arnott, M.J.B. Cartigny, M.A. Clare, F. Felletti,  
383 J.A. Covault, S. Girardclos, E. Hansen, P.R. Hill, R.N. Hiscott, A.J. Hogg, J. Hughes  
384 Clarke, Z.R. Jobe, G. Malgesini, A. Mozzato, H. Naruse, S. Parkinson, F.J. Peel, D.J.W.  
385 Piper, E. Pop, G. Postma, P. Rowley, A. Sguazzini, C.J. Stevenson, E.J. Sumner, Z.  
386 Sylvester, C. Watts, J. Xu, 2015, Key future directions for research on turbidity currents  
387 and their deposits: *Journal Sedimentary Research*, v. 85, p. 153-169.

388

389